ANALECTA
PRAEHISTORICA
LEIDENSIA 47

PUBLICATION OF THE P.J.R. MODDERMAN STICHTING/
FACULTY OF ARCHAEOLOGY
LEIDEN UNIVERSITY

EXCERPTA ARCHAEOLOGICA LEIDENSIA II

EDITED BY
HANS KAMERMANS AND CORRIE BAKELS

LEIDEN UNIVERSITY 2017

Series editors: Corrie Bakels / Hans Kamermans

Editor of illustrations: Joanne Porck

ISSN 0169-7447
ISBN 978-90-822251-4-3

Contents

Neutron-based analyses of three Bronze Age metal objects: a closer look at the Buggenum, Jutphaas and Escharen artefacts

Hans Postma, Luc Amkreutz, David Fontijn, Hans Kamermans, Winfried A. Kockelmann, Peter Schillebeeckx and Dirk Visser

Three important Bronze Age copper-alloy artefacts from the permanent exhibition of the National Museum of Antiquity in Leiden (NL) have been studied by neutron-based methods. These artefacts are known as the Buggenum sword, the Jutphaas dirk, and the Escharen double axe. All three objects have been studied with neutron resonance capture analysis (NRCA), a non-destructive method to determine the bulk elemental compositions. The Buggenum sword is also studied with time-of-flight neutron diffraction (TOF-ND) giving additional information about crystalline properties and internal material structures, and neutron tomography (NT), showing details of the construction of this sword and voids inside the material. The composition of the Jutphaas dirk is compared with the compositions of two other dirks belonging to the group of six Plougrescant-Ommerschans (PO) ceremonial dirks. The Escharen double axe, identified as being of the Zabitz type, variant Westeregeln, is a rare object in the Low Countries. It is compared to finds from Central Europe. The results for all three objects are discussed with regards to their archaeological contexts and their relation to other finds.

1 Introduction

There is a strong need to develop analytical methods for studying object compositions that do not require the taking of samples and are thereby entirely non-destructive. Methods that use neutrons for such analyses hold great potential. This contribution will show the results of a number of neutron-based analytical techniques for three special objects, which are too unique for destructive sampling.

The large penetrability of neutrons through matter allows determination of bulk properties of objects. Neutrons can react in different ways with nuclei. A neutron can be captured by a nucleus, producing a new (compound) nucleus with one more neutron in a highly excited state, which in most cases will decay by emitting gamma radiation promptly. This gamma radiation can be detected by a dedicated set of special detectors. The probability of a capture reaction as a function of neutron (kinetic) energy shows peaks, which are known as resonances, and which are related to highly excited states of the compound nucleus. The energies at which these resonances occur are specific to the isotopes of the elements. Hence, elements of an object can be recognized in a neutron capture spectrum, often even already during data taking, on the basis of resonance energies. The numbers of counts in resonance peaks contain information about the amounts of the elements. To derive elemental amounts requires careful data analysis after the measurements. Knowledge about resonance parameters, neutron beam properties, and properties of detectors must be available for this analysis. Alternatively, calibration data can be used. The phenomenon of resonances in a capture spectrum is the basis of neutron resonance capture analysis (NRCA).

The energy of neutrons can be determined with the time-of-flight (TOF) method, which requires a pulsed source of neutrons to be able to measure the time (t) neutrons need to travel a known distance (L) to the object. That is, the pulsed neutron source gives a start pulse and the gamma detector the stop pulse for timing a neutron capture event in the object. This method gives the velocity $v = L/t$ of the neutron and thus its kinetic energy $E = \frac{1}{2}mv^2$, in which m is the neutron mass. The unit used for neutron energy is the electronvolt (eV)[1].

The neutron energy can be determined with the expression: $E = 5227.039(L/t)^2$, where E is in eV, L in meter and t in μsec. The TOF neutron capture spectrum shown in figure 1 is that which was obtained for the Escharen double axe, one of the objects under study (see below for further details).

The NRCA method as applied to archaeological objects has been developed at the GELINA facility by a team from the University of Technology in Delft (NL) and the EC-JRC Institute in Geel (B).

Neutron diffraction (ND) makes use of the wave properties of neutrons and uses scattering from regular crystalline planes in the material. ND provides information about the metal and mineral phase compositions, for example contents of different copper-tin phases in a copper alloy, as well as the microstructural properties, such as locked-in strains and other remnants of the working history of the alloy. To allow the matching of the wavelength with lattice dimensions, the

energy of the neutrons must be low, in practice in the range from thermal neutrons (0.024 eV) up to a few eV. As the neutron energy can be determined by the time-of-flight method, these two components make up the time-of-flight neutron diffraction (TOF-ND) method. This kind of research has been carried out at the ISIS facility of the Rutherford-Appleton laboratory in Harwell (UK).

In neutron tomography (NT), a two-dimensional image obtained by transmission of thermal neutrons through an object is registered with a scintillator plate viewed by a CCD camera. By making a large number of such 2D radiographies with the object viewed under a large number of angles, and by applying dedicated computer algorithms, a 3D-data set of the object is obtained. With these data it is also possible to cross the object in different requested directions, produce slices, and also fly-through video presentations. The Buggenum sword has been subjected to neutron tomography at the FRM-II research reactor in Garching (GE).

During exposure to neutrons objects may become radioactive. The amount of activation depends on the neutron flux, their energy and irradiation time. Particularly (sub)-thermal neutrons activate objects. Since such neutrons are not needed for NRCA, they are removed from the beam with the aid of filters. In addition the detection of capture events is rather large, thus, objects are left with low activation after neutron capture measurements. Neutron diffraction and neutron tomography measurements are carried out with thermal neutrons. Consequently larger activations may exist after such measurements, notably for NT, which requires taking data for long periods with the object under a large number of orientations. For this reason it is advisable to carry out NRCA, ND and NT in this order. This approach was taken for the Buggenum sword in the course of the ANCIENT CHARM[2] collaboration (Gorini and Kamermans 2011). Waiting periods are observed to let the activity die out to a sufficiently low level before returning objects to the owner, applying very stringent official international rules for activities of objects in the public domain. For most of the reported experiments waiting periods were short, less than one day for NRCA experiments, of the order of a few days for neutron diffraction, and considerably longer for neutron tomography.

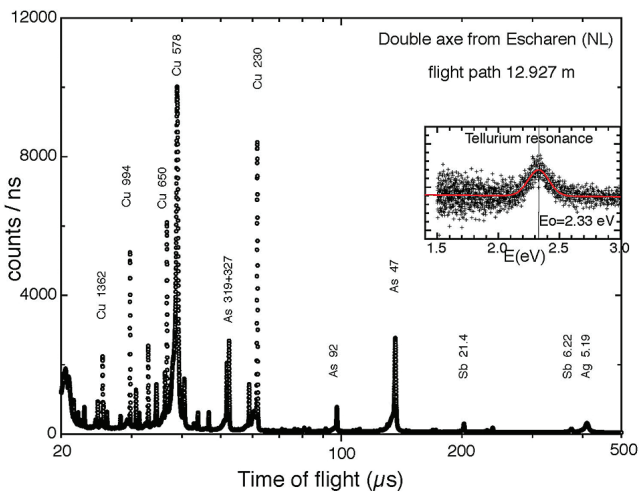

Figure 1 Time-of-flight capture spectrum of the Escharen double axe obtained at the GELINA facility in Geel (BE) using a beam with flight path of 12.927 m between the pulsed neutron source and the center of the axe. Resonances are indicated by the element symbols and resonance energies derived from the time-of-flight

2 Copper alloy objects from the National Museum of Antiquity (NMA)

The following three artefacts from the prehistoric permanent exhibition collection of the National Museum of Antiquities (NMA) in Leiden (NL) have been studied: the so-called Buggenum sword (RMO inventory no. l 1999/12.1), the Jutphaas dirk (RMO inventory no. f 2005/3.1) and the Escharen double axe (RMO inventory no. K 1992/9.1). Their names are related to find locations in The Netherlands (fig. 2). These are well-preserved objects for which taking samples or polishing parts of the surface for study purposes is not allowed.

Figure 2 Find locations of the three objects from the Dutch National Museum of Antiquities

All three neutron-based analytical techniques have been applied to the Buggenum sword. The composition of the Buggenum sword, resulting from the NRCA data and most of the TOF-ND data, is published in a technical paper (Postma *et al*. 2010). In the current paper additional information is given including the tomography results and a comparison with other Middle Bronze Age objects.

The Jutphaas dirk is one of the six known Plougrescant-Ommerschans (PO) dirks. These are very similar in shape and layout, although there are differences in size and composition. The Jutphaas dirk is the smallest of the group (see Butler and Sarfatij 1970/1; Fontijn 2001). Neutron resonance capture measurements of the Jutphaas dirk show a detailed elemental composition, which can be compared with the compositions of two other Plougrescant-Ommerschans dirks from Beaune and Oxborough, and the Kimberley dirk of a very similar shape, as published by Stuart Needham (1990). These artefacts are most likely ceremonial weapons dated to the Middle Bronze Age. Till recently five PO dirks were known. The latest addition was found at Rudham (UK, as yet unpublished).

The Escharen double axe is also a ceremonial object. It is recognized as a Zabitz type axe, which is a rare object in The Netherlands (Butler 1995/6, 167-70). It can be compared with a series of Zabitz axes described by Kurt Kibbert (1980, 35-54). The composition of the Escharen axe has been determined by neutron resonance capture, allowing a comparison with the list of 27 Zabitz axes given by Kibbert although their compositions are considerably less well determined. The Zabitz axes are from the very Early Bronze Age or from the end of the preceding copper Age.

3 Some essentials of neutron-based methods and available equipment

In this section some basic aspects of the three neutron-based methods, mentioned in the introduction, are briefly discussed. Since neutrons are unstable particles (half-life 882 s), they are not directly available and must be produced by nuclear reactions. This requires research reactors or dedicated particle accelerators.

3.1 Neutron resonance-capture analysis (NRCA)

The capture cross-section[3] of a single, isolated s-wave neutron-resonance can be approximated by the a Lorentzian shape[4]:

$$\sigma_\gamma(E) = \frac{\sigma_\gamma^o}{1 + x^2}, \text{ in which } x=2(E–E_0)/\Gamma. \quad (1)$$

Herein E is the energy of the incident neutron, E_o the central energy of the resonance, Γ its width at half-height, and σ_γ^o the maximum value of the cross-section at the central energy of the resonance. If only gamma-ray emission occurs after neutron absorption the width is the sum of the partial widths of the neutron entrance and gamma-ray emission channels: $\Gamma = \Gamma_n + \Gamma_\gamma$. To determine an elemental amount in a sample, it is important to know the area A_γ of the resonance. It is given by:

$$A_y = 4{,}097.10^6((A+1)/A)^2 g_J \Gamma_n \Gamma_y / E_0 \Gamma, \text{ (in units barn.eV).} \quad (2)$$

A is the mass number and g_J a factor depending on the combination of the neutron and nuclear spins.

Before continuing the discussion about analysing NRCA spectra, it is important to mention three effects which modify the observed resonance profile. First the thermal motion of nuclei should be mentioned, which broadens the resonance and makes it resemble a Gaussian curve, at least around its central energy. The far-out wings of the resonance have still a Lorentzian shape. This so-called Doppler broadening effect widens and lowers the resonance peak, but its area remains the same.

The second effect modifying a resonance spectrum concerns the reduction of the intensity of the neutron beam when it traverses an object. There is a reduction due to potential scattering. This reduction is in first approximation energy independent. In the region of a resonance the neutron flux will be strongly reduced near the resonance centre and less at its wings. Consequently the capture count rate of resonance (μ) of an element will be reduced by an energy-dependent factor $F_\mu(E)$, which can be calculated on the basis of the total cross section and the amount of the element. Integrated over the resonance peak, the count rate is reduced by a F_μ, which is known as the self-shielding factor.

The third modification is the possibility of scattering (once, twice or even more) of a neutron in the object before it is captured. At each scattering the neutron loses an amount of energy depending on the scattering angle. As a consequence each resonance is accompanied by a wide structure at its high-energy side, while its size and shape depend on the thickness and form of the object. It may be partially underneath a resonance peak, especially in the case of low-energy resonances. Such a scattering-capture structure should first be subtracted from the resonance spectrum before the number of counts in a resonance peak can be derived. This may require dedicated analysing codes. For the applications described in this paper an empirical analysis often suffices. Figure 3 is an example taken from the resonance capture spectrum of the Jutphaas dirk, showing the 230-eV resonance of copper with its scattering-capture structure. For this resonance the peak and the scattering-capture structure can be well separated. For resonances at higher energies the scattering-capture structure moves away from the resonance becoming a lesser problem. For

resonances at lower energies the structure moves underneath the peak and thus the separation becomes more difficult especially for resonances of a few eV.

In the case of a homogeneous and flat object the number density (n_X) of an element (X) in the object can be obtained by dividing the number of counts (N_μ) in the peak of a resonance (μ) by a number of parameters, that is:

$$n_x = N_\mu/\varepsilon_\mu F_\mu A_{y,\mu} a_\mu \Omega \Phi(\varepsilon_\mu). \quad (3)$$

$\Phi(E_\mu)$ is the time integrated neutron flux at resonance energy, Ω is the area of the object illuminated by the beam, a_μ the isotopic abundance, $A_{\gamma,\mu}$ the theoretical capture area, F_μ the self-shielding factor, and ε_μ the efficiency to detect a capture event. The latter depends on the detector arrangement. With this expression it is possible to determine the amount of an element in an object in an absolute way. However, it requires knowledge of a large number of factors, some of which are hard to determine. It requires absolute monitoring of the neutron flux entering the sample. An added difficulty is that the shielding factor depends on the areal density, i.e. the total amount of the element per unit area of the object.

The efficiency for detecting capture events in particular is very difficult to determine precisely. In addition, it may even vary between resonances of the same nuclide, because their prompt gamma ray spectrums can be different. Furthermore, in archaeology objects have rarely simple flat shapes, and thus applying equation 3 can only be approximately valid, or requires an integration procedure.

For this reason the so-called double ratio method has been introduced for analysing archaeological objects. In this method the ratio of the count rates in two resonances (λ and μ) of two elements (X and Y) of an object is compared with the same ratio of a calibration sample of known composition. This method gives the weight fraction W_X/W_Y of two elements X and Y by the expression:

$$\frac{W_X}{W_Y} = K^{cal}_{\mu,\lambda}\frac{F_\lambda N_\mu}{F_\mu N_\lambda}, \quad \text{with} \quad K^{cal}_{\mu,\lambda} = \left(\frac{F_\mu N_\lambda W_X}{F_\lambda N_\mu W_Y}\right)_{cal}. \quad (4)$$

In the double ratio methods some of the parameters mentioned with equation 3 cancel to a high degree, and therefore it is not necessary to know them. The cancelling of detector efficiencies and flux ratios are especially important assets of this method.

Many elements have several resonances available for the analysis. For instance; copper has suitable resonances at 230, 650 and 1150 eV, and tin at 38.8, (45.7) and 111.0 eV. Hence

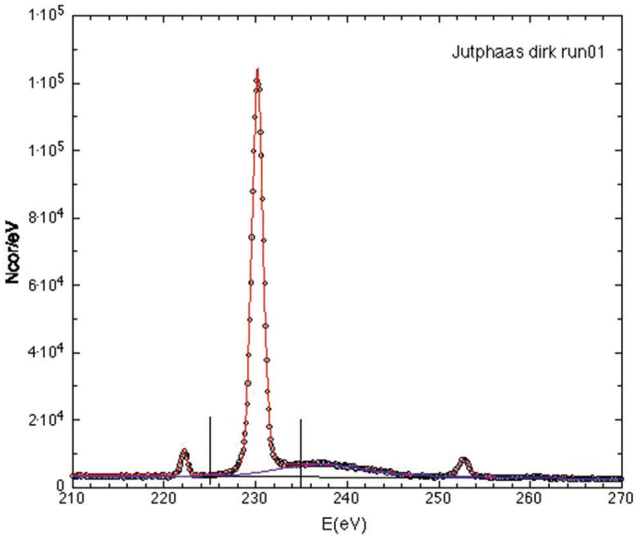

Figure 3 Part of the capture spectrum of the Jutphaas dirk showing the 230-eV copper resonance with its scattering-capture structure. The subtraction of the latter is important for determining the number of counts in the resonance peak itself. In addition two weaker resonances in this plot are from tin (222 eV) and arsenic (253 eV)

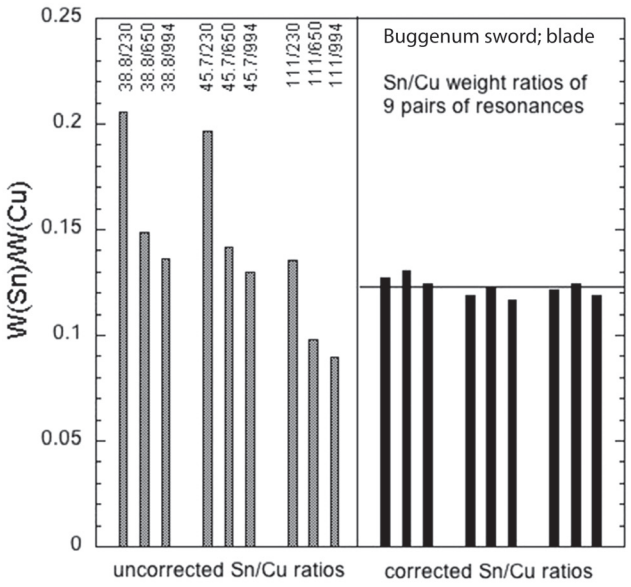

Figure 4 Bar plot of weight ratios of tin with respect to copper for nine pairs of resonances for the blade of the Buggenum sword. At the left side uncorrected ratios and at right side ratios corrected for self-shielding factors valid for the mean Cu-thickness, which is obtained with the variation method (Postma *et al*. 2010)

to determine the tin to copper weight ratio in a bronze object six (or nine) pairs of resonances can be used. Analysing the experimental weight ratios without accounting for self-shielding, that is with all *F*-factors assumed to be one, the obtained weight ratios of these pairs of resonances are quite different as is shown in the left side of the bar plot in figure 4 for the blade of the Buggenum sword. Using *F*-factors for the copper and tin resonances, the weight ratios can be made equal; see right side of figure 4.

This procedure leads to a variation method in which the weight ratios $R = W_{Sn}/W_{Cu}$ of several pairs of resonances are calculated from the data by varying the *F*-factors for copper and tin as a function of the areal density of copper and tin till the lowest value of the variance $\Sigma(R-\langle R\rangle)^2$ has been reached; $\langle R\rangle$ is the mean value of the ratio for all used resonance pairs. Figure 5 shows, as an example, the result of this variation method applied to the Jutphaas dirk. For clarity this figure is limited to two sets of curves for the mean ratio (left *y*-axis) and the variance (right *y*-axis) for two fixed values of the amount of tin while the amount of copper is varied (*x*-axis). With other chosen values of the amount of tin, the minimum values of the variance are higher than those shown in the figure. If the ratio of the amounts of tin and copper valid for the minimum of the variance curve corresponds with the derived value of $\langle R\rangle$ at the left *y*-axis, then this is a validation of the result. This is the case of the curves related to a tin amount of 0.30 g/cm^2, but not for the curves related to 0.25 g/cm^2 of tin. In addition the first case has the lowest value of the variance.

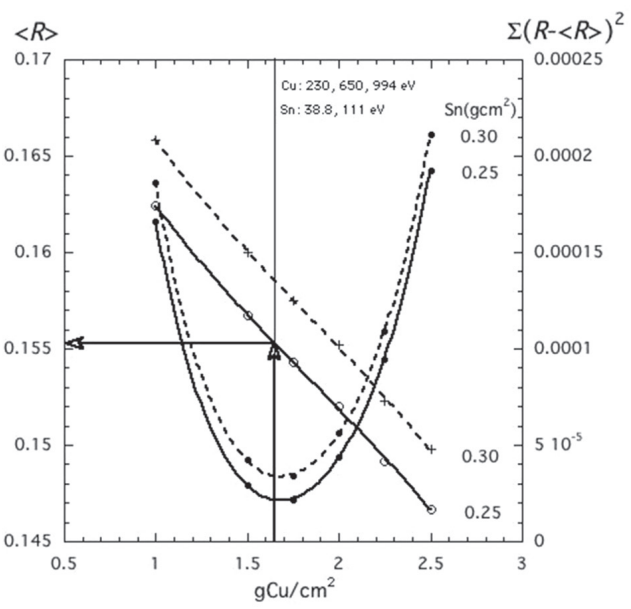

Figure 5 Example of the variation method as applied for the Jutphaas dirk and based on 6 pairs of resonances using copper resonances at 230, 650, 994 eV and tin resonances at 38.8, 111 eV

More technical details about NRCA and analyzing procedures can be found in Postma and Schillebeeckx (2010; 2017) and Schillebeeckx *et al*. (2012).

The reported neutron resonance capture experiments have been carried out at the pulsed neutron source of the GELINA facility which is operated by the Joint Research Centre of the European Commission in Geel (B). At this facility neutrons are produced in short pulses by stopping bursts of electrons from a 150 MV accelerator in a uranium disk with a maximal repetition rate of 800 Hz. These neutrons are partly moderated in two small, water-containing vessels above and below this uranium disk. Beam tubes are viewing these containers to allow neutrons to reach measurement stations at different distances from the neutron source. Two of these stations, made available for NRCA, are equipped with C_6D_6 detectors for detecting gamma radiation. These detectors have very good timing properties and are insensitive to neutrons. The nominal lengths of these flight paths are 12 and 28 m.

More information about the GELINA facility are given by Mondelaers and Schillebeeckx (2006).

3.2 Time-of-flight neutron diffraction (TOF-ND)

The wave property of neutrons makes it possible to study crystalline structures of objects by the diffraction method (ND). This method is non-destructive, like NRCA, as the neutrons penetrate through coatings and corrosion layers deep into centimeter-thick materials, thus providing information about the interior parts of an object. Metal and mineral phase compositions, texture and strain analysis can be performed, and hence information about working steps and fabrication techniques can be derived (Siano *et al*. 2003). The wavelength depends on the energy of the neutrons. In case of a polychromatic, pulsed neutron source it is possible to determine the neutron energy by the TOF-method. The ISIS facility at the Rutherford Appleton Laboratory in the UK, based on a spallation neutron source, provides a number of facilities for TOF-ND. The ENGIN-X instrument of the ISIS facility has been used for analysis of the Buggenum sword. The instrument has a collimated beam of cold neutrons and provides a set of two large area (of more than 2 m^2 in total) ZnS scintillation neutron detectors, with radial collimation viewing the sample. The two detector banks are at 90º on either side of the object. Each bank has 1200 ZnS(^{6}Li) scintillators. Therefore it allows for TOF-ND to be carried out at small volumes down to 2×2×2 mm^3 size and inside objects. The diffraction spectra, one for each detector bank, are analyzed by the Rietveld method (Kockelmann *et al*. 2006).

3.3 Neutron tomography (NT)

The principle of neutron tomography is rather straightforward. A wide beam of low-energy neutrons transmits through an object, and produces a two-dimensional (2D) radiography of the object on a scintillator screen. The scintillator converts the neutron image into a visible-light image, which is registered with a CCD camera. Repeating this collection of a radiography a large number of times (a few hundred), with the object in different orientations, and using dedicated software programs it is possible to reconstruct from these CCD-images tomographic data sets, hence a three-dimensional (3D) presentation of the object. This kind of work is typically carried out at research reactors providing high intensity, low-energy neutron beams. The high penetration of neutrons in materials makes the study of the internal structures of objects possible, even features inside thick metal parts which X-rays cannot penetrate easily.

An example of a tomography facility is ANTARES at the FRM-II reactor at the Hans-Leibnitz Zentrum in Garching near München (Germany) (Calzada *et al*. 2009). This facility was used to produce tomographic data sets of the Buggenum sword.

The ANTARES facility for radiography and tomography uses neutrons moderated in a vessel containing liquid deuterium cooled to 25 K and placed near the core of the FRM-II reactor, thus providing a spectrum of cold neutrons that peaks at 1.6 Å with a long tail (of thermal and fast neutrons) at the high energy side[5]. The neutrons from this moderator travel through a collimating opening of diameter *D* (constituting a 'pinhole') installed 4.5 m from the cold source. Then the neutrons travel through 'flight tubes', filled with helium gas in order to avoid scattering of neutrons by air to the sample position at 12 m from the pinhole.

Thereafter, these neutrons traverse the object, which is mounted on a manipulator. With this manipulator the object can be moved in vertical and horizontal directions and it can be rotated over 360°. Behind the object is a scintillator with a large area to produce a two-dimensional image of the object. This scintillator consists of zinc sulphide and contains lithium-fluoride. The reaction products (^{3}H and ^{4}He) from capture of neutrons by the ^{6}Li isotope generate a light flash in the zinc sulphide. A CCD camera which is installed away from the neutron beam and which views this scintillator via a mirror under 45°, and an optical lens stores this image. To reiterate, radiographies are recorded with the object in many orientations to produce a tomographic data set.

The resolution of the images depends to a large extent on the divergence of the neutrons defined by the pinhole, that is on a typical length *L* and diameter *D*. ANTARES can be operated with two values of *L*/*D*, namely 400 or 800. The best resolution is obtained with the larger value at the cost of a lower intensity of the neutron beam.

4 Description of the Buggenum Sword

4.1 History of the discovery

The bronze sword from Buggenum was dredged from an old bedding of the river Meuse near Buggenum in the province of Limburg, the Netherlands in 1964. It was unknown to archaeologists until the early 1990's. The finder, Mr. Peters, kept it in his possession until 1999 when it was purchased by the National Museum of Antiquities in Leiden. Butler and Fontijn made a detailed study of the object (Butler and Fontijn 2007; Fontijn 2002, 166-168).

4.2 Description

The sword is an all-metal object of unknown, presumably bronze, composition. The length is 68.5 cm, at the shoulder of the hilt it is 3.8 cm wide, and it weighs 920 grams. Figure 6 shows a photo of the sword. The hilt has an oval cross-section with four ring-like ridges, it is slightly tapered and it has an intricate decoration. There are "running in-and-out spirals" between the rings of the hilt and the pommel. The nearly circular pommel is also beautifully decorated; at the top with connected spirals as well, and underneath with three rings of incisions. Furthermore, the short projection above the pommel is decorated with incisions. In the region where the hilt goes over into the blade it is decorated with incised lines and four little circles, which look like rivets. Two of them may actually replicate rivets but the other two seem to be genuine rivets hidden in the line-shape decoration. No traces of seams (brazing or soldering) could be recognized at the "omega shaped" connection of hilt and blade, or near the pommel. The way the blade and hilt are connected could therefore only be guessed. The blade is sharpened, but there is no evidence it was used as a weapon. The whole sword shows the skilled workmanship of the smith who made this object. Halfway along the blade a dent is visible, which suggest that the sword may have been bent. Whether this was done deliberately, as sometimes happened with metal objects during the Bronze Age (cf. Fontijn *et al*. 2012), or was a result of the dredging, is unknown.

4.3 Place in European context

Butler and Fontijn (2007) concluded that we are dealing with a so-called full-hilted decorated sword (German: *Vollgriffschwert)* of the Central European *Vielwulstschwert*-variety ('multi-ribbed grip sword'), sharing traits of the *Dreiwulstschwert* of type *Erding* ('three-ribbed grip sword') as defined by Von Quillfeldt (1995, 142-188; see also Müller-Karpe 1961, 7-48, and further references cited in Butler and Fontijn 2007). Two other *Dreiwulstschwerte* have been studied by Marianne Mödlinger with X-rays and with NRCA (Mödlinger 2007).

On typo-chronological grounds, the object could be dated to the Middle Bronze Age B in the Dutch chronology (more precisely, its latter part, Ha A 1, *c*. 1300 to 1100 BC; Butler and Fontijn 2007, 310). Our inventory of similar finds in Europe showed that this type of sword is uncommon in Western Europe in general, and in the Low Countries in particular (Butler and Fontijn 2007, fig. 27.4 and 27.5). It is known in large numbers in Central Europe, however. On typological grounds, Butler and Fontijn (2007, 305-7) deduced that the Buggenum sword was probably produced in Bavaria. This implies that the sword reached the Netherlands via long-distance exchange.

The sword is in splendid condition and nothing indicates that it was ever used in battle. In comparison to other swords found in the Low Countries and adjacent West Germany, the Buggenum sword stands out both by its richly decorated grip, and its unused and undamaged condition. This seems to be a sword with an exceptional biography that was used for display and ceremonial purposes only. It was argued that it ended its life by being deliberately deposited in the river Meuse or its back swamps where it remained for thousands of years until it was found by the dredgers (Butler and Fontijn 2007, 313-4). This long stay in a waterlogged environment explains its excellent condition of preservation. A further study of Bronze Age metalwork finds in this part of Europe showed that the riverine context of the Buggenum sword is not exceptional: this particular zone of the Meuse has so far yielded many Bronze Age swords, the majority of which must have been deliberately deposited there by Bronze Age communities (Fontijn 2002, fig. 8.11). Full-hilted swords, however, are rare among the river finds, let alone lavishly decorated swords. In this aspect, the Buggenum sword, then, surely is an exceptional case. This made a follow-up on Butler and Fontijn's investigations worthwhile, and when the opportunity arose to do new research on technological properties of precious prehistoric artefacts within the framework of the ANCIENT CHARM project, the Buggenum sword was an obvious candidate.

4.4 Research questions

Given the opportunity to apply the newly developed neutron-based techniques for material characterization, and the new possibilities of tomography for studying the mechanical construction in particular, the Buggenum object seemed interesting, as Butler and Fontijn suspected that the sword was made in two separate parts which were joined together later in the production process (Butler and Fontijn 2007, 301). This idea was based on parallels from Central Europe, where casting moulds for full-hilted swords are known where hilt and blade were separate, as well as from X-ray inspections of swords (Mödlinger 2007). It should be remarked though, that a joint between hilt and blade is not immediately apparent when one studies the lower parts of the hilt.

5 Neutron based measurements of the Buggenum sword

In the framework of the ANCIENT CHARM project (Gorini and Kamermans 2011) the Faculty of Archaeology (Leiden

Figure 6 Photo of the Buggenum sword (photo National Museum of Antiquities RMO, Leiden)

University), the section Radiation, Detection and Medical imaging (RD&M) of the Faculty of Applied Sciences (Delft University of Technology), and the National Museum of Antiquities (NMA) in Leiden (NL), owner of the Buggenum sword, decided to study the Buggenum sword, however only with non-destructive methods. The goal was to obtain information about its elemental bulk composition, including a number of minor and trace elements, its construction and the way it may have been manufactured and worked on. Three types of neutron-based measurements were carried out in the following order: i) neutron resonance capture analysis (NRCA) at the GELINA facility, ii) time-of-flight neutron diffraction (TOF-ND) at the ISIS facility, and iii) neutron tomography (NT) at the Garching research reactor. The GELINA facility was also used to get a radiographic picture of the hilt in order to understand the NRCA data of the hilt. The NRCA and TOF-ND measurements and data of the Buggenum sword are described and discussed in a technical paper (Postma *et al*. 2010).

5.1 NRCA results

The neutron resonance capture measurements were carried out at eight locations on the blade, at four places on the hilt and one location where hilt and blade are connected, using a beam with 2.2 cm diameter at half-height (Postma *et al*. 2010). The data were analyzed with the double ratio method explained in section 3.1 and are presented as weight ratios with respect to the major element copper. Analysed elements concern copper, tin, antimony, arsenic, silver, indium, cobalt and zinc. Since tin and copper each have three resonances, Sn/Cu weight ratios of nine pairs of resonances could be obtained. Without correcting for self-shielding, these ratios differ considerably; see left side of figure 4. When correcting for self-shielding in a variation approach a mean value of the tin to copper weight ratios was obtained together with a mean thickness of the blade in gram copper per cm^2; see right side of figure 4. The derived mean thickness has been used for correcting weight ratios of the other elements to copper with proper self-shielding factors. The weight ratios are plotted in figure 7 for the 13 locations of the Buggenum sword. The vertical line in this figure goes through the middle of the "Omega" location where blade and hilt are connected and where run 4AB has been carried out. The locations of the runs 5AB through 5HI, 1AH and 1BG are on the blade from the tip to the connection with the hilt. 1CF concerns the hilt plus tang of the blade and 1DE the hilt only just below the pommel.

The weight ratios at the eight positions of the blade show little or no variation. The measurement at the hilt shows a larger variation at the various locations. In table 1 the weight fractions averaged for the eight positions of the blade, and the weight fractions at the positions on the hilt just underneath the pommel are quoted in columns 2 and 5.

In archaeological papers amounts of components are usually given in weight%. For reasons of comparison, the fractions have been converted into weight% in the two A-columns of table 1, assuming that no other components exist in the metal. Elements like nickel and iron may also occur in bronze artefacts in several per cent as residue from the copper smelt. Lead is often added in the melt of artefacts in considerable amounts. But these elements were not observed in the capture spectra of the Buggenum sword with estimated upper limits U given in the ratio columns of table 1. Taking these upper limits into account as ½(U±U), weight fractions of the detected elements change slightly as is shown in the B-columns of table 1.

The tin-to-copper ratios of blade and hilt differ by about 20%, which shows that both parts of the Buggenum sword are made from different melts. Given their errors the ratio values of the impurities Sb, As, Ag, In, and Zn do not differ for hilt and blade. The values for Co are somewhat outside their error ranges, however, the analysis of Co is based on one wide and small resonance within a complicated part of the resonance spectrum and is therefore rather difficult.

It can be concluded that the copper used for both parts is likely from the same origin.

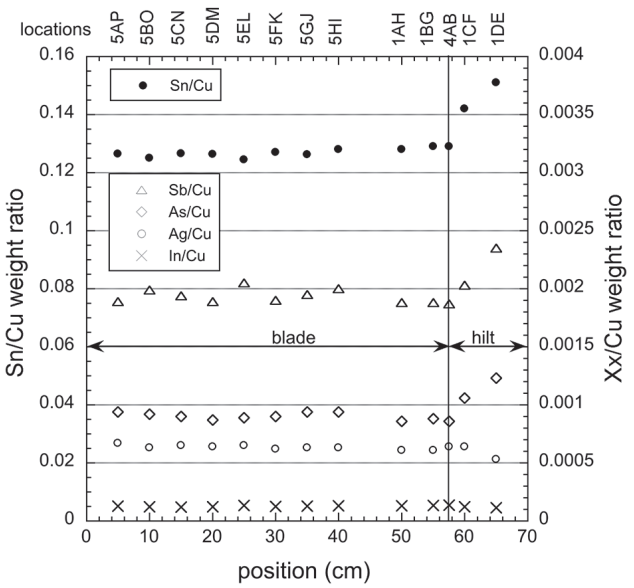

Figure 7 Weight ratios of elements observed for the Buggenum sword with respect to copper plotted as a function of the distance (*x*-axis) along the sword from the tip of the blade to the top of the pommel. Symbols of the runs given at the top of the figure are from figure 1 of Postma *et al*. 2010

Element	Blade			Hilt		
	Ratio to Cu	Wt% A	Wt% B	Ratio to Cu	Wt% A	Wt% B
Cu	1*	88.44 ±0.15	86.60 ±1.27	1*	86.40 ±0.15	85.77 ±0.49
Sn	0.1250 ±0.0018	11.06 ±0.15	10.82 ±0.21	0.1510 ±0.0020	13.05 ±0.15	12.96 ±0.17
Sb	0.00194 ±0.00010	0.172 ±0.017	0.168 ±0.019	0.00235 ±0.00020	0.203 ±0.017	0.202 ±0.017
As	0.00090 ±0.00010	0.080 ±0.009	0.078 ±0.009	0.00123 ±0.00020	0.106 ±0.017	0.105 ±0.017
Ag	0.00063 ±0.00004	0.056 ±0.004	0.055 ±0.004	0.00053 ±0.00008	0.046 ±0.007	0.046 ±0.007
In	0.000128 ±0.000007	0.011 ±0.001	0.011 ±0.001	0.000116 ±0.000020	0.010 ±0.002	0.010 ±0.002
Co	0.000136 ±0.000030	0.012 ±0.003	0.012 ±0.003	0.000046 ±0.000010	0.004 ±0.001	0.004 ±0.001
Zn	0.0020 ±0.0005	0.177 ±0.044	0.173 ±0.044	0.0021 ±0.0003	0.181 ±0.026	0.180 ±0.026
Ni	<0.020		0 - 1.74	<0.0045		0 - 0.38
Fe	<0.001		0 - 0.08	<0.0005		0 - 0.04
Pb	<0.027		0 - 2.3	<0.012		0 - 1.0

* by definition

Table 1 Compositions of the blade and hilt of the Buggenum sword quoted as weight ratios to copper and in weight% fractions; columns A without including upper limits for Ni, Fe and Pb, and columns B including these elements in calculating the weight fractions

5.2 Results of TOF-ND measurements

Neutron diffraction measurements have been carried out on 15 locations of the Buggenum sword, four locations on the hilt, one in the 'omega' area (where blade and hilt meet), five on the rib of the blade and four on the edges of the blade. All measurements showed that its tin-bronze is mainly in the alpha phase[6] with small amounts of the delta phase in accordance with the formation of the eutectoid in the as-cast bronze. Figure 8 shows the diffraction pattern obtained at two locations, one on the rib and the other on the edge. The alpha lines of the diffraction spectra observed at the rib are very broad and somewhat structured; see figure 8a. The general broadening is considered to be due to Cu-Sn heterogeneities in the metal, corresponding to dendritic tin segregation during solidification. The three-pronged structure can be related to mainly three alpha-phases with locally different compositions. The alpha lines are sharp at the edges of the blade due to homogenization of the bronze by repeatedly reheating, annealing and hammering for sharpening and strengthening the edges; see figure 8b.

In general, the delta phase fractions are small except for four of the rib positions with delta phase fractions of 4 – 6 wt% and the two rivets with 2.0 and 1.6 wt%. In all other positions the delta phase fractions are below 1 wt%.

The lattice constant of the bronze varies mainly by the addition of tin. With Vegard's rule and calibration data the apparent tin content can be obtained (Siano *et al*., 2006). Correcting for the contribution of minor elements, obtained from NRCA, to the lattice parameter gives the following results for the Sn/Cu weight ratios:

hilt just under the pommel: apparent Sn/Cu ratio 0.155, corrected 0.1515,
rib of the blade: apparent Sn/Cu ratio 0.132, corrected 0.129,
edges of the blade: apparent Sn/Cu ratio 0.142, corrected 0.139.

The NRCA results for the hilt and blade are 0.151 (just under the pommel), respectively 0.125, as averaged over the full blade.

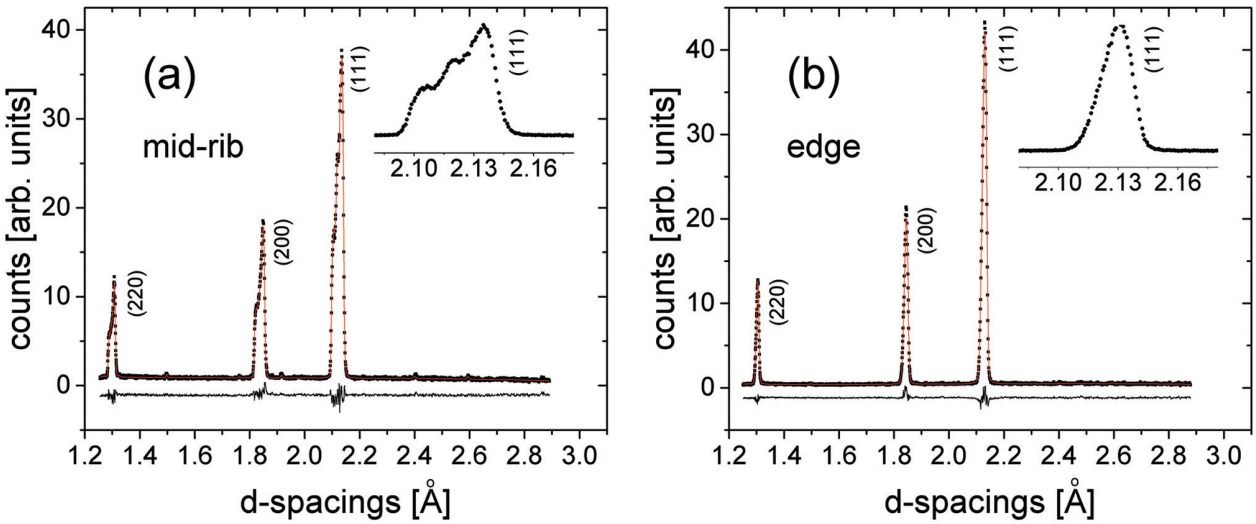

Figure 8 Diffraction pattern obtained at two locations of the Buggenum sword, one on the middle of the rib (a) and the other on the edge (b)

Copper and its alloys may contain elements or compounds, which do not dissolve and which can be detected by neutron diffraction because of their specific diffraction lines, for instance lead and CuS. The TOF-ND results of the Buggenum sword do not show such lines. It is concluded that this sword contains less than 0.5 weight% of lead.

5.3 Results of neutron tomography

Neutron tomography has been carried out on the Buggenum sword using the ANTARES facility of the FRM-II reactor in Garching (Ge) described in section 3.3.

Both the blade and the hilt have been investigated in order to learn more about the mechanical construction and quality of the object. From a large number of radiographic 2D-images taken with the Buggenum sword rotated in small steps over 360º, tomographic data sets of three parts of the sword have been produced. These data sets can be used to produce movies and slices as cross sections of the sword. For instance, one movie shows the rotating sword hilt with its external decorations in backlight. In two tomography movies the hilt is traversed in two perpendicular directions, which makes it possible to study the construction of the hilt and the way the tang of the blade was inserted into the hilt. Hence, these data show important details of the quality of the sword, for instance how the sword blade and hilt were joined, allowing a classification and comparison to other swords. From the tomography data sets two slices through the object are presented in figure 9. Both slices are through the middle of the sword and show the full length of the hilt; part A of this figure is in the plane of the blade and B is perpendicular to this plane. Together they give a good presentation of the construction of the way the tang of the blade is positioned inside the hilt. The tang of the blade does not penetrate fully into the hilt, but stops just over halfway inside the hilt. This was also concluded from a radiographic image of the hilt made with a beam of gamma radiation at the GELINA facility in order to be able to interpret the NRCA data. In figure 10, showing details of the hilt, it looks as if four rivets have been used to connect the blade to the hilt, however, two of them were suspected to be only part of the incised decoration of the sword. On the tomographic slice (fig. 9A) only two rivets are visible and thus the other two on the photograph are indeed imitation rivets.

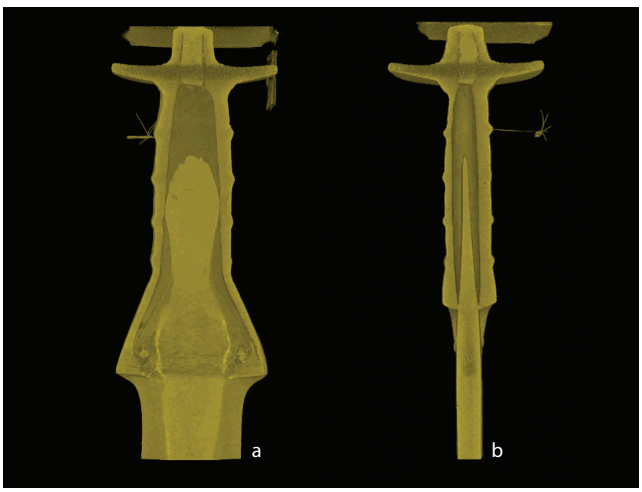

Figure 9 Two slices as cross sections of the Buggenum sword produced from the tomographic data sets; (A) the cross section of the hilt in the plane of the blade and (B) perpendicular to it

Figure 10 Photo of the hilt of the Buggenum sword (photo National Museum of Antiquities RMO, Leiden)

Another observation made possible by the tomographic data sets is the occurrence of a wide hole in the top of the pommel; see figure 9. This hole may have been essential for fixing the inner part of the mould. After casting the hole may have been important to remove the inner part of the mould used for casting the hilt. After constructing the sword, the hole could then have been closed with a plug, as is clearly visible from the tomography.

The two sets of tomographic data of the blade mainly show the homogeneity of the material. The blade is clearly a solid piece of metal with only a few small voids visible in the images.

5.4 Conclusions about the Buggenum sword

The Buggenum sword is an all-metal product from the Middle Bronze-Age and probably originates from the Danube region. Based on the different tin contents, the blade and hilt are from different casts both close to eutectic tin-copper. It has very precisely executed incised decorations and the absence of wear or damage implies that it may only have been used for ceremonial purposes. Nevertheless, the apparent work on the edges of the blade and the sturdy, solid construction of the sword show that it has been made as a potentially functional weapon, not as a showpiece with a ceremonial purpose only.

6 Description of the Jutphaas dirk

6.1 History of the discovery

The Jutphaas dirk was found in 1946 or 1947 during dredging operations for the extension of a shipyard harbour in the Jutphaas county area just south of the city limits of Utrecht (Butler and Sarfatij 1970/1). While at first it was not recognized as such, the artefact decorated for years the room of the young nephew of the finder. When it became clear that it was apparently one of a very rare group of ceremonial weapons it was sold to the National Museum of Antiquities.

6.2 The Plougrescant-Ommerschans dirks

The Jutphaas dirk is one of six known ceremonial dirks of very similar design, including the recent find in Durham (UK), which is not yet described in the literature. Most of the dirks are around 70 cm, and show only slight differences in their execution. However, the Jutphaas dirk with its length of 39 cm is considerably smaller. In the literature this remarkable group of ceremonial objects is known as the Plougrescant-Ommerschans dirks, named after two find locations, one in France and the other in the Netherlands (Butler and Bakker 1961). Although very similar, the Jutphaas dirk is not an accurate miniaturization of the large specimens (Butler and Sarfatij 1970/1). Nevertheless the resemblances are so striking that it is assumed all may have derived from the same workshop (Butler and Sarfatij 1970/1; Fontijn 2001). This is of importance since these objects were dispersed over quite a large region, with two ending up in England, two in France (Brittany and Burgundy) and two in the Netherlands. Furthermore, there are no signs for hafting of these swords; the edges are not sharpened and they are simply too large to serve as weapons. They are dated to the Middle Bronze Age, *c*. 1500-1350 BC, maybe somewhat later (Needham 1990).

6.3 Elemental compositions

So far the only information about the elemental composition is from Butler and Sarfatij (1970/1), mentioning a qualitative measurement by J.N. Lanting (BAI, Groningen, NL) based on X-ray spectroscopy. It is said to be a tin-bronze with only a trace of nickel. This result does not allow a comparison with elemental analyses of the Oxborough and Beaune dirks presented by Stuart Needham (1990). Therefore neutron resonance capture measurements were carried out with the Jutphaas dirk using beam No.5 of the GELINA facility with flight path length of 12.116 m and a beam diameter of about 7.5 cm at the sample position. Figure 11 shows the Jutphaas dirk in front of the two C_6D_6 detectors of the NRCA equipment. It is mounted on an aluminium plate for easy transport and safe handling. Overlap filters of bismuth, cadmium and sulphur were inserted early in the beam. The measurements concern the hilt and the tip of this dirk. The resulting elemental compositions from this analysis are given in table 2 in weight % with estimated errors largely based on systematic trends. For tin the errors are of the order of 1 wt%. For copper the errors are compounded from the errors of the other elements. Iron, nickel and lead at the bottom section (tip) of the Jutphaas dirk could not be determined satisfactorily by NRCA due to limited beam time for this run. Due to the beam filters used during these experiments, it was not possible to derive the amounts of bismuth and sulphur. These elements are expected to occur in small amounts at most.

Stuart Needham (1990) reported analyses of the Oxborough and Beaune dirks and three other objects, indicated as the Essex/Kent rapier, the Kimberley dirk and Wandle Park spearhead. Multiple samples were taken from each of these objects with a 1 mm drill. Samples were taken to obtain reliable averaged compositions in three regions (hilt, middle and tip) of the Oxborough and Beaune dirks. The samples were dissolved in *aqua regia* for inductively coupled plasma (ICP) spectroscopy using the equipment of the Mineralogy Department of the National History Museum (London, UK). The resulting compositions of the Oxborough, Beaune and Kimberley dirks are quoted in table 2 except for gold, bismuth, cadmium, manganese and phosphor which were below their detection limits of respectively 0.003, 0.01, 0.007, 0.003 and 0.02 wt%. The errors for the various elements are said to be of the order of 1 % for copper and 5 % for tin. The precisions for the minor and trace elements worsen from about 10 % to 50 % at their respective detection limits. Lead is not detected by NRCA; the detection limit is about 0.5 wt%. Sulphur included in the analyses given by Stuart Needham is well below 0.1 wt%, however, it cannot be detected by NRCA. Indium detected by NRCA occurs in very small amounts in the Jutphaas dirk. This element is probably not seen with ICP spectroscopy.

Table 2 includes the minor elements silver, arsenic, cobalt, iron, nickel, and antimony usually occurring in Bronze-Age copper. These elements dissolve in copper during the

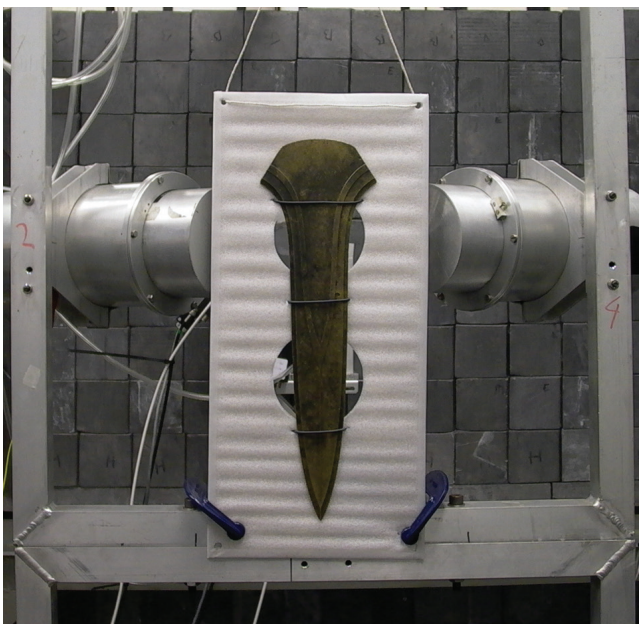

Figure 11 The Jutphaas dirk in front of the two C_6D_6 detectors of the NRCA equipment (photo National Museum of Antiquities RMO, Leiden)

	Ag	As	Co	Cu	Fe	In	Ni	Pb	S	Sb	Sn	Zn
Jutphaas												
Top	0.0160	0.297	0.035	85.46	0.022	0.0028	0.34	< 0.5		0.106	13.50	0.105
	±0.0008	±0.015	±0.002	±0.15	±0.002	±0.0002	±0.03			±0.003	±0.15	±0.006
Tip	0.0124	0.226	0.033	86.07	–	0.0028	–	< 0.5		0.114	13.39	0.153
	±0.0011	±0.017	±0.002	±0.15		±0.0002				±0.003	±0.15	±0.014
Oxborough												
Hilt	0.018	0.35	0.027	83.7	0.035		0.54	0.168	0.05	0.09	13.8	0.03
Mid	0.017	0.36	0.028	85.8	0.040		0.54	0.148	0.04	0.10	13.9	<0.007
Tip	0.017	0.34	0.029	84.4	0.036		0.53	0.170	0.04	0.10	13.5	<0.007
Beaune												
hilt **repair**	0.023	0.27	–	81.6	0.214		0.039	3.85	0.04	0.03	4.96	7.58
mid	0.019	0.23	0.026	84.6	0.023		0.544	0.138	0.09	0.10	13.6	0.012
Tip	0.020	0.22	0.025	85.4	0.029		0.547	0.138	0.09	0.12	13.7	<0.007
Kimberley												
	0.013	0.33	0.031	84.2	0.201		0.733	0.13	0.07	0.08	14.8	<0.009

Table 2 Compositions in weight% of three Plougrescant-Ommerschans and the Kimberley dirks from Stuart Needham (1990), and NRCA measurements

smelting process. This is probably also true for iron, but it cannot be excluded that some iron is present due to taphonomic processess. Lead occurs as globules in copper. In small quantities it may also come from the smelting process. Larger amounts of lead such as the 3.85 wt% in the hilt side of the Beaune dirk are presumably added while melting the metal for the casting process.

The indicated parts of Jutphaas and Oxborough dirks and the middle and tip sections of the Beaune dirk are remarkably identical tin bronzes with very similar amounts of tin and made from copper with nearly identical impurity patterns. The averaged value for tin of these seven measurements is 13.63 wt% with a variance of 0.06 wt%. It seems likely that these dirks are made from the same metal production by the same smith, probably at the same location.

The hilt section of the Beaune dirk is a tin-lead-zinc bronze produced by adding considerable amounts of tin, lead and zinc to the copper melt. Stuart Needham (1990) assumes that the hilt section of the Beaune dirk is a modern cast-on repair. However, the copper used for this repair contains the minor elements silver, arsenic and antimony. On the other hand, bronzes with large amounts of zinc do not occur in the Bronze Age (cf. Henderson 2000, 212 ff.). To get zinc into copper requires difficult procedures not known in the Bronze Age.

The zinc results quoted in table 2 have to be discussed in more detail. In the case of the Oxborough dirk the zinc values for the three regions differ considerably, that is, 0.03 wt% at the hilt region and below the detection limit of 0.007 wt% for the middle and the tip. Similarly for the middle and tip positions of the Beaune dirk the values are 0.012 wt% and below 0.007 wt%. However, the zinc contents of the two regions of the Jutphaas dirk are larger and of the order of 0.13 wt%. This variation in zinc contents may be related to the sample taking, or measurement techniques. Another reason for these differences might be related to the casting process. Zinc has a boiling temperature of 907 ºC, which is near the melting temperature of bronze. Thus zinc has a high vapour pressure during the melting and casting process, and as a consequence part of the zinc may evaporate. Thus it is difficult to draw conclusions on the basis of the zinc contents.

The tin content of 14.8 wt% of the Kimberley dirk is larger and outside the range of values for the three Plougrescant-Ommerschans dirks. Its nickel content is also larger, but the other minor element compositions, Ag, As, Co, Fe and Sb, are similar considering the errors for these elements. Zinc again is below the detection limit. It seems reasonable to conclude that the Kimberley dirk is from a different production but probably made from a similar kind of copper alloy in terms of metal compositions.

The column bar plot of figure 12 shows weight ratios of elements with respect to copper for the three Plougrescant-Ommerschans and the Kimberley dirks as averages of the

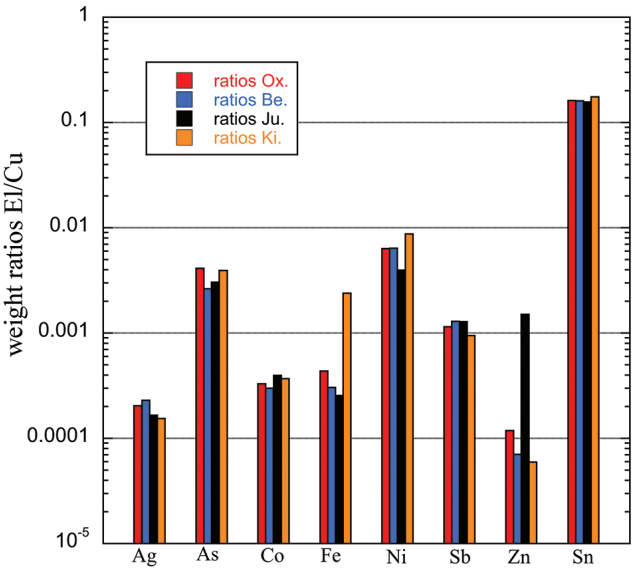

Figure 12 Weight ratios of elements with respect to copper for the Oxborough, Beaune, Jutphaas and Kimberley dirks. See the text for discussion

regions, not including the hilt region of the Beaune dirk. It is a useful plot to appreciate the equality of the compositions of the three Plougrescant-Ommerschans dirks and some of the differences with the Kimberley dirk.

6.4 Concluding remarks concerning the Jutphaas dirk

The Jutphaas dirk belongs to the group of ceremonial Plougrescant-Ommerschans giant dirks. The composition of the Jutphaas dirk is very similar to those of the Oxborough and Beaune (unrepaired part) dirks. These results strengthen the supposition that this set of dirks shares many similarities and perhaps a common origin. This supposition is visually convincingly underlined by the similarities in shape and design. The current study adds to this that there are also very distinct similarities in composition, hence leading to choices concerning the manufacture of these giant dirks. These similarities underline that the group of swords may have been devised and made in a relatively short amount of time and possibly in the same place. This is of importance for studying the reasons behind the fabrication of these impressive ceremonial objects.

7 The Escharen double axe

7.1 History of the discovery

This axe is a very rare find from the Netherlands. In the published information by Butler (1995/6, 167-70) this double axe was said to have been found accidentally at a depth of circa 1 meter during the building of a garage in the village of Escharen near the city of Nijmegen (NL). In a series of notes about the village of Escharen it is mentioned that the Escharen double axe has been found in the mid-seventies by Cor Emons during the building of his garage at the Beersemaasweg 51 (Esters Heem, bodemvondsten 2015/6). He dispatched it in a bucket with junk matter in order to pick it up later. That happened a decade later in 1986 when it was given to a flea market. There it was sold to Jo van den Hoogen. He was sure the object was ancient and tested the composition. As the shining bright orange copper emerged from underneath the patina he was sure and went out of his way to re-trace where it was found, eventually locating the finder through a newspaper advertisement. Thanks to the intervention of Van den Hoogen the Escharen double axe found its way to the Dutch archaeological community and eventually to the National Museum of Antiquities.

The find area is locally known as ‘De Bullen’. Such a name is typical in that area for describing wet meadowlands, and the area was known to flood relatively quickly. According to Van den Hoogen, the find may have been situated on a piece of elevated land close to the Beersemaasweg, it is clear that its deposition, burial or abandonment occurred in a dynamic area that was characterized by water and floods covering the axe with layers of sediments. Moreover, Escharen itself is situated near the confluence of a small stream called the Raam and the river Meuse. These wet locations are classical sites where deposition of metal objects took place in later prehistory (see Fontijn 2002).

The axe is currently on display at the National Museum of Antiquities as part of its permanent prehistoric exhibition. Figure 13 shows a picture of this axe. It is 36.9 cm long, the widths of the two blades at the ends are 7.5, respectively 7.35 cm; it weighs 980 grams. It has a hole in the middle, which appears to be too narrow for hafting this axe for a practical purpose. Butler (1995/6) recognized it as a Zabitz type double axe, variant Westeregeln. It is of interest to determine the elemental composition of the Escharen axe and see whether this agrees with the compositions of the double axes reported by Kibbert (1980). Presumably these double axes are ceremonial objects.

The Escharen double axe is in good shape except for two small damages (see fig. 14); one is a set of cuts (with a saw or a file) at its edge done by Jo van den Hoogen for inspecting the composition. The other damage is in the same place and clearly done with a bore apparently to get a sample. The conic hole has a maximum diameter of 2 mm and has a maximum depth of 2 mm. It is not known who took the sample at this location and no result of an analysis is known.

Figure 13 The Escharen double axe (photo National Museum of Antiquities RMO, Leiden)

7.2 Elemental composition

The composition of the Escharen double axe has been determined with neutron resonance capture measurements using beam No.5 of the GELINA facility with a flight path length of 12.927 m to the sample position and a beam diameter of about 70 mm. The centre of the beam coincides roughly with the middle of one of the wings of the double axe. Bismuth, cadmium and sulphur have been used as neutron filters to keep the activation during the run as low as possible. The collected TOF spectrum is shown in figure 1 presented in the introduction. In this figure several of the resonances are marked with their element symbols and central resonance energies. There are a number of strong resonance peaks related to copper, while other marked peaks are from arsenic, antimony and silver. Already during the data taking it was clear that this double axe is made from some sort of arsenical copper. Other weak peaks, identified after the run, are related to silver, gold, cobalt and, interestingly, tellurium. Upper limits of count rates are estimated for some resonances expected to occur for tin, iron, cobalt, nickel and indium, elements which often occur in copper-based artefacts.

Weight fractions of the elements with respect to copper were obtained by the usual analysing methods of NRCA. The variation method in which several pairs of resonances of copper and antimony (or arsenic) are used, and in which the copper thickness is used as a variable parameter, did not work well, as has been experienced with tin-bronzes, for instance in the case of the Buggenum sword; see section 3.1. The amounts of arsenic and antimony are clearly too small for this method to work properly for the Escharen double axe. In this case variations in count-rate ratios depend mainly on the difference of shielding factors for the copper resonances. The obtained apparent copper thickness is in the broad range of 4 to 7 g. Cu/cm^2. Using the specific density of copper this leads to a thickness of order of 5 to 8 mm, which is consistent with the averaged thickness of 6.5 ± 0.4 mm derived from measurements with a micrometre carried out at five locations of the part of the artefact illuminated by the beam.

Figure 14 The Escharen double axe with damages for inspecting the composition, and to get a sample (photo National Museum of Antiquities RMO, Leiden)

element to copper	weight ratios and errors	element	weight % and errors
		Cu	98.4 ± 0.5
Sb/Cu	0.00122 ± $6x10^{-5}$	Sb	0.120 ± 0.006
As/Cu	0.00747 ± 0.00040	As	0.735 ± 0.004
Ag/Cu	0.00043 ± $4x10^{-5}$	Ag	0.044 ± 0.004
Au/Cu	$21x10^{-6}$ ± $4x10^{-6}$	Au	0.0021 ± 0.0004
Co/Cu	$29x10^{-6}$ ± $3x10^{-6}$	Co	0.0029 ± 0.0003
Te/Cu	0.00015 ± 0.00001	Te	0.015 ± 0.001
Sn/Cu	<$12x10^{-6}$	Sn	< 0.001
Zn/Cu	<0.00018	Zn	< 0.018
Fe/Cu	<0.0005	Fe	< 0.5
Ni/Cu	<0.0086	Ni	< 0.8
Pb/Cu	<0.005	Pb	< 0.5
In/Cu	<$10x10^{-6}$	In	< 0.001

Table 3 The composition of the Escharen double axe as based on neutron resonance capture data

Find location	Sn	As	Sb	Ag	Ni	Bi	Pb	Fe	S
Hämerten	0.03	1.5	0.10	trace	trace	0.07		0.15	
Petersberg	trace	0.05	trace	trace	trace	trace			
Pyrmont	0	0	0	0	0	trace		0.1/0.04	
Ketzin	trace	1.05	0.05	0.01	0.01	0.015			
Altenburg	trace	1	trace	trace	trace	trace			0.47
Worms	trace	0.40	0.50	0.80	0.80	trace		0.10	
Westeregeln	0	0.52	0.03	<0.01	<0.01	0.005			
Börssum	0.04	1	0.1	trace	trace	0.005			
Nienburg	0.03	1	0.05	trace	trace			0.40	
Grasrup-Hölsten 1	trace	0.49	0.09	<0.01	0.019	0.009	0.02		
Grasrup-Hölsten 2	0	0.23	0.07	0.013	0	0.001			
Ellierode	"pure copper"								

Table 4 Minor elements in wt% and "trace" elements of twelve Zabitz axes, Westeregeln variant, taken from Kibbert (1980)

The composition of the Escharen double axe, as derived with NRCA, is quoted in table 3 in weight %. The errors are mainly determined by uncertainties of the analysis, notably in the variance of ratios of pairs of resonances (*e.g.* nine in the case of antimony). Table 3 also includes elements for which upper limits could be estimated. In the case of nickel and lead the upper limits are rather large, 0.8 and 0.5 wt%, due to the low sensitivities to observe these elements in neutron capture experiments.

The very weak resonance peak at 2.33 (±0.01) eV observed in the analysis of the Escharen axe (see fig. 1) could only be related to tellurium isotope ^{123}Te with a resonance at 2.334 eV as quoted in the literature. The estimated amount of tellurium in the Escharen axe is 0.015 wt%. Tellurium has not been seen in earlier NRCA experiments, and as far as we know, also not mentioned in the literature about elemental analyses of copper-alloy artefacts.

The Escharen double axe is made from arsenical copper with relatively low values for arsenic and antimony, and with some very small (trace) amounts of silver, gold, cobalt and tellurium.

7.3 Comparison with other Zabitz axes

Kibbert (1980) collected information about 32 double axes of the Zabitz type and divided them into three groups according to their weights; 1) above 2 kg and up to 3.5 kg, 2) a group between about 1 to 1.6 kg, and 3) a group below 1 kg. He recognized three variants named "Cochem", "Flonheim" and "Westeregeln". These variants correlate quite well with the three weight groups. The Westeregeln axes are undecorated and shaped like an hourglass. Butler (1995/6) recognized the Escharen double axe as a Zabitz axe, Westeregeln variant. With its weight of 980 gram it is a relatively heavy member of this variant. There are two other heavy double axes of the Westeregeln variant mentioned by Kibbert (1980), one from Petersberg weighing about 1000 g and one from Hämerten of 1490 g. The lightest double axe (Gastrup-Hölsten 2), accepted by Kibbert as a Westeregeln variant, weighs 278 g.

Table 4 shows the elemental compositions of 11 Zabitz double axes, Westeregeln variant, taken from Kibbert (1980, 291). They can either be considered as pure copper artefacts (Bad Pyrmont and Ellierode) or they are made from arsenical copper with small amounts of arsenic ranging from 0.23 to1.5 wt% (average 0.7). The Escharen axe (0.73 wt% arsenic) fits well in this group. Quoted amounts of antimony range from 0 to 0.1 with an average value of 0.07 wt%. The Escharen axe has a somewhat larger value. Tin is observed in three of these axes with amounts of about 0.04 wt%, it is mentioned as trace elements, or tin is apparently below the detection limit indicated as "zero". Amounts of other elements, Ag, Ni and Bi, are in most cases not given but are also indicated as "trace" or "zero". Lead is in one case (Altenburg) mentioned, iron in three cases (Hämerten, Bad Pyrmont and Nienburg) with maximum value of 0.40 wt% and sulphur in only one case (Altenburg) as 0.47 wt%.

Other Zabitz axes of the variants Cochem and Flonheim have similar compositions with at most small or trace amounts of Sn, As, Sb, Ag, Ni and Bi.

It is apparently, after Otto and Witter (1952), generally accepted that arsenical copper is obtained by smelting fahlore, (ideal formula $Cu_{12}(As/Sb)_4S_{13}$), and is noted in the literature as "fahlore copper". The Zabitz double axes are clearly made from arsenical copper. Therefore some sulphur is expected to occur in these artefacts. Unfortunately, sulphur could not be detected with neutron resonance capture because of the sulphur disk inserted into the beam to remove high-energy neutrons from the beam to reduce activation of the Escharen axe. Sulphur is reported only for the Altenburg axe, Westeregeln variant.

Fahlore minerals contain considerable amounts of arsenic and antimony. However, all 27 analysed Zabitz double axes contain small or very small amounts of these elements. This may be related to low-temperature smelting of fahlore. On the basis of experiments by R.G. Thomas, as reported by Budd as unpublished data, smelting of fahlore below about 900 °C produces a semi-copper product with less than 2 wt% of arsenic. At higher temperatures up to 8 wt% is expected (Budd *et al*. 1992, Budd 1993). The low-temperature smelting could have been carried out at the mining site. Further reduction of the arsenic and antimony contents, and also sulphur, may have occurred during melting of the fahlore copper for casting the artefacts.

Tellurium is a very rare element chemically related to sulphur and selenium. As a first thought one might think that the observed tellurium can be an impurity replacement of sulphur in fahlore. However, there are two factors that make this hypothesis unlikely. Firstly, the atomic radius of tellurium is much larger than that of sulphur; 143 pm compared to 103 pm for sulphur. Secondly, the occurrence of tellurium in the earth crust is very small; about 0.001 mg/kg compared to 350 mg/kg for sulphur. Hence, geological processes must have been very favourable for tellurium to replace sulphur in fahlore. Tellurium has been found as poly-metallic compounds in minerals. It was discovered in Europe in the gold mining area of Romania (Spiridonov 2013) and recently in the Erzgebirge (Förster 2004) as intermetallic compounds with gold and silver.

7.4 Find locations and origin of the copper of the Zabitz axes

The find locations of Zabitz double axes, Westeregeln variant, are shown on the map of figure 15. The locations of the axes of this variant are mainly in Central-Germany, in a region north of the Harz between the rivers Weser and Elbe, with a cluster near Magdeburg. Therefore, the copper used for the Zabitz axes may have come as a semi-product from the Harz where large amounts of sulphide ores occur in its western mountains (Lüders *et al*. 1993).

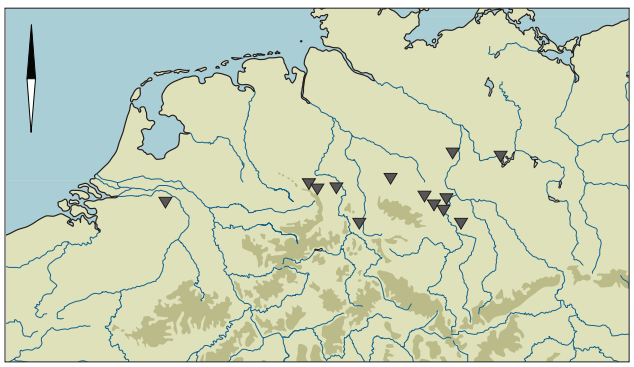

Figure 15 Map showing the find locations of Zabitz type double axes, Westeregeln variant. After Butler 1995/6, figure 5

However, the Erzgebirge might be another possible mining area for the copper used for the Zabitz axes because of the occurrence of tellurium recently shown to exist as Ag_2Te (Hessite) in the nearby Erzgebirge (Förster 2004). Tellurium also occurs in combination with gold for instance as $Cu(Au,Ag)Te_4$ in the Carpathian region where considerable gold deposits exist (Spiridonov 2013). But this region is likely too far away to be a source of copper for the Zabitz double axes.

7.5 Conclusions concerning the Escharen axe

The Escharen double axe is a rare find in the Netherlands. It was recognized as a Zabitz type axe of the variant Westeregeln. Its composition corresponds well with other axes of this type. The Escharen double axe is very likely a long-distance export from a region in Central-Germany near the city Magdeburg and a little west of it. The fahlore copper used for the production of this type of axes may have come from the Harz, but the Erzgebirge is also a reasonable candidate for this copper because of the occurrence of tellurium. It is of interest to analyse some of the Zabitz double axes again to check the occurrence of gold and tellurium. The find location of the axe indicates it was most probably a deposition in or near a wet context.

In the Low Countries, double axes are largely absent and both in shape and use (its non-functional hafting) the object seems out of the ordinary – having a shape that largely lacks counterparts in both previous, contemporary and later material culture in Lower Rhine Basin (cf. Butler 1995/6, 167-70; Fontijn 2002, 66). Among contemporary copper-alloyed objects, arsenic objects have been detected particularly for objects dated to the early Bronze Age (in the Dutch chronology, cf. Butler and Van der Waals 1966). The NRCA results show the Escharen one is not as uncommon in composition as it is in shape. More comparative research on bronze compositions is needed, however, to verify this.

8 General remarks and conclusions

Summing up, the above described analyses show that two of the artefacts (the Buggenum sword and Jutphaas dirk) are tin-bronzes with several impurity elements like antimony, arsenic, silver, indium, cobalt and zinc presumably from the smelting process of copper minerals or recycling of that metal.

NRCA demonstrates that the composition of the smaller Jutphaas dirk clearly belongs to the group of aggrandized ceremonial weapons to which it bears such strong similarities. It fits in well with previous ideas that all these ceremonial dirks were produced in one workshop. The Escharen double axe is an arsenic-bronze with quite a different impurity spectrum of antimony, silver, gold, cobalt and tellurium. It is a long distance exchange object coming from a region in central Germany. Its copper may have been obtained by smelting fahlores mined in nearby regions like the Harz and/or Erzgebirge.

The tomography of the Buggenum sword gives valuable information about the mechanical construction of the object in general and in particular of the way the tang of the blade is positioned inside the hilt.

Thus the three objects from the National Museum of Antiquity, discussed in this paper, originate from three different regions each with different mining areas. The current paper demonstrates that non-invasive, non-destructive techniques, such as NRCA, TOF-ND and NT are very suitable for investigating the composition and discussing the origin of these objects. While there are of course certain aspects, or dangers, such as over-exposure and mounting of the objects in experimental equipment to consider, it is clear that from a museal perspective these techniques offer viable alternatives to destructive sampling as has been the case for the Escharen double axe. The integrity of the objects remains unaltered, while, in contrast to for example handheld XRF-measurements, a much higher level of information is retrieved. It is subscribed by the National Museum of Antiquities and may be considered one of the major outcomes of the Ancient Charm collaboration, that these techniques form an important step forward in the way valuable objects from both public and private collections may be researched in a ‘sustainable’ manner. It is stressed here that for most archaeological questions and composition analysis these techniques suffice and are to be chosen instead, or before destructive sampling takes place. Having said that, a major point remains that these analyses should in the future be embedded in research programs with a distinct archaeological question at its core (see Amkreutz 2014). While it is interesting that these techniques work well for archaeological objects they form a means to an end. The authors hope that this contribution may to some extent have ‘shown the potential’ of neutron-based analyses.

Acknowledgments

The NRCA experiments have been carried out under an agreement between the EC-JRC in Geel (BE) and the Faculty of Applied Sciences of the Delft University of Technology (NL).

Part of the research mentioned in this paper has been carried out under the EU FP6 Ancient Charm project, funded by the European Commission under the contract No. 15311.

Neutron beams have been made available for free at the GELINA, ISIS, and FRM-II facilities. The authors want to

acknowledge the staffs for their skillful operation of these facilities and the kind hospitality experienced at the EC-JRC in Geel (BE), the Rutherford-Appleton Laboratory in Harwell (UK), and the FRM-II Reactor institute in Garching (GE). The authors also wish to thank the National Museum of Antiquities in Leiden (RMO) for their cooperation in the research undertaken within and outside of the Ancient Charm programme with regard to these objects. Thanks are also extended to the Groningen Institute of Archaeology for sharing information and expertise with us, in particular to Hannie Steegstra and the late dr. Jay Butler. Last but not least, we like to thank Jessica Palmer for improving our English.

Notes

1 1 eV is equivalent to 1.6×10^{-19} joule, this is the energy an electron gains when accelerated over 1 volt.

2 The European FP6 project ANCIENT CHARM used non-destructive neutron-based techniques and studied a number of cultural heritage objects from Hungary, Italy and The Netherlands. The goal of the physicists in the project was to develop a 3-D imaging technique based on epithermal neutron absorption and the archaeologists wanted to use the various methods to characterize the heritage objects and, in one case, suggest methods for preservation or restoration.

3 As common in nuclear physics reaction strengths are expressed in effective areas, the cross sections in units of barn equal to 10^{-28} m^2.

4 The Lorentzian shape $1/(x^2+1)$ of a reaction channel is based on the Heisenberg uncertainty relation (energy x time), while in a statistical process like thermal motion the distribution is well described by the Gaussian function $\exp(-y^2)$.

5 The terms "thermal" and "cold" are somewhat confusing. Neutrons in thermal equilibrium within the reactor are named "thermal". Their mean energy is about 0.025 eV. Neutrons coming from a moderator at a low temperature, which is placed close to the reactor core, are named "cold".

6 Alpha and delta phases occur during the solidification of tin-bronze after casting. They are equilibrium phases in the copper-tin system. Both phases have face-centred cubic crystal structures. Copper with up to about 10 atomic % of tin solidifies in the alpha phase with tin distributed randomly in the copper lattice; its Pearson symbol is cF4. The delta phase occurs at the eutectic point. Its composition is $Cu_{41}Sn_{11}$ with Pearson symbol cF416.

References

Amkreutz, L.W.S.W. 2014. From Vollgriffschwert to lightsaber. In: C.C. Bakels; K. Fennema; J.F. Porck and M. Wansleeben (eds), *We discovered that … Times are a-changin and much stays the same. Contributions on the occasion of the retirement of Hans Kamermans*, Leiden, 13-18.

Budd, P. 1993. Recasting the Bronze Age. *New Scientist* 23 October 1993, 33-37.

Budd, P., D. Gale, A.M. Pollard, R.G. Thomas and P.A. Williams 1992. Notes. The early development of metallurgy in the British Isles. *Antiquity* 66, Issue 252, 677-686.

Butler, J.J. 1995/6. Bronze Age metal and amber in the Netherlands, part II:1. Catalogue of flat axes, flanged axes and stopridge axes. *Palaeohistoria* 37, 159-243.

Butler J.J. and J.A. Bakker 1961. A Forgotten Middle Bronze Age Hoard with a Sicilian Razor from Ommerschans (Overijssel). *Helinium* 1, 193-210.

Butler J.J. and D.R. Fontijn 2007. Spiralling from the Danube to the Meuse: the metal-hilted sword from Buggenum (Netherlands, Limburg). In: Ch. Burgess, P. Topping and F. Lynch (eds). *Beyond Stonehenge, Essays in the bronze age in the honour of Colin Burgess*. Oxford Books, 301-315.

Butler, J.J. and H. Sarfatij 1970/1. Another Bronze Ceremonial Sword by the Ploughescant-Ommerschans Smith. *Berichten van de Rijksdienst voor het Oudheidkundig Bodemonderzoek* 20-21, 301-309.

Butler, J.J. and J.D. van der Waals 1966. Bell beakers and early metal-working in the Netherlands. *Palaeohistoria* 12, 41-139.

Calzada, E., F. Gruenauer, M. Mühlbauer, B. Schillinger, M. Schulz 2009. New design for the ANTARES-II facility for neutron imaging at FRM II. *Nuclear Instruments and Methods in Physics Research* 605, 50–53.

Esters Heem, bodemvondsten 2015/6. http://www.estersheem.nl/bodemvondsten/bronzen-bijl

Fontijn, D.R. 2001. Rethinking ceremonial dirks of the Plougrescant-Ommerschans type. Some thoughts on the structure of metalwork exchange. In: W.H. Metz, B.L. van Beek and H. Steegstra (eds), *Patina. Essays presented to Jay Jordan Butler on the occasion of his 80th birthday*, Groningen/Amsterdam, 263-280.

Fontijn, D.R. 2002. *Sacrificial Landscapes, Cultural biographies of persons, objects and 'natural' places in the Bronze Age of the Southern Netherlands, c. 2300-600 BC*. PhD thesis, University of Leiden.

Fontijn, D.R., L. Theunissen, B. van Os and L. Amkreutz 2012. Decorated and 'killed'? The bronze sword of Werkhoven, *Analecta Praehistorica Leidensia* 43-44, 203-211.

Förster, H.J. 2004. Mineralogy of the Niederschlema-Alberoda U-Se-polymetallic deposit, Erzgebirge, Germany. II: Hessite, AG2Te, and native Te (?), the first tellurium minerals. *Neues Jahrbuch für Mineralogie - Abhandlungen* 180, 2, 101-113.

Gorini, G. and H. Kamermans with R. Cattaneo, E. Perelli Cippo, A. Pietropaolo and M. Tardocchi, C. Andreani, B. Adembri, M.L. Arancio, P.A. Caroppi, M. de Pascale, G. Festa, D. Malfitana, R. Senesi, A. M. Giusti, A. P. Recchia, S. Porcinai, K.T. Biró, K. Dúzs, Zs. Hajnal, T. Belgya, Zs. Kasztovszky, Z. Kis, L. Szentmikósi, A.Kirfel, J. Jolie, R. Schulze, P. Kudejova, P. Schillebeeckx, A. Borella,, T. Materna, D. Fontijn, L. Amkreutz, S. Scholten, C.W.E. van Eijk, V.R. Bom, M.C. Clarijs, M.C. Moxon, H. Postma, E. Godfrey, W. Kockelmann, P. Radaelli, N.J. Rhodes, E.M. Schooneveld and D.Visser. 2011. Neutron-based Analysis for Cultural Heritage Research. Results of the Ancient Charm project. In: W. Börner and S. Uhlirz (eds). *Workshop 14. Archäologie und Computer. Kulturelles Erbe und Neue Technologien*. Museen der Stadt Wien – Stadtarchäologie, Wien, 211-233.

Henderson, J. 2000. *The Science and Archaeology of Materials. An investigation of inorganic materials*. London/ New York: Routledge.

Kibbert, K. 1980. Die Äxte und Beile im mittleren Westdeutschland I. *Prähistorische Bronzefunde* IX-10.

Kockelmann, W., S. Siano, L. Bartoli, D. Visser, P. Hallebeek, R. Traum, R. Linke, M. Schreiner and A. Kirfel 2006. Applications of TOF neutron diffraction in archaeometry. *Applied Physics* A83, 175-182.

Lüders, V., K. Stedingk and H.J. Franzke 1993. Review of Geological Settings and Mineral Paragenesis. *Monograph Series on Mineral Deposits* 30, Gebrüder Bornträger, Berlin-Stuttgart, 4-11.

Mödlinger. M. 2007. *Herstellung und Verwendung bronzezeitlicher Schwerter aus Österreich*, PhD Thesis Universitaet Wien.

Müller-Karpe, H. 1961. *Die Vollgriffschwerter der Urnenfelderzeit aus Bayern*. Münchner Beitr. Vor- u. Frühgesch. 6 München.

Mondelaers, W. and P. Schillebeeckx 2006. GELINA, A neutron time-of-flight facility for high-resolution neutron data measurements. *Notiziario Neutroni e Luce di Sincrotrone*, 11(2), 19-25.

Needham, S. 1990. Middle Bronze Age ceremonial weapons: new finds from Oxborough, Norfolk and Essex/Kent. *The Antiquaries Journal* vol. LXX, part II, 239-252.

Otto, H. and W. Witter 1952. *Handbuch der ältesten vorgeschichtelichen Metallurgie in Mitteleuropa*, Leipzig.

Postma, H., L. Amkreutz, A. Borella, M. Clarijs, H. Kamermans, W. Kockelmann, A. Paradowska, P. Schillebeeckx, and D. Visser 2010. Non-destructive bulk analysis of the Buggenum sword by neutron-resonance capture analysis and neutron diffraction. *Journal of Radioanalytical and Nuclear Chemistry* 283, 641-652.

Postma, H. and P. Schillebeeckx 2010. Neutron Resonance Capture and Transmission Analysis. In: R.A.Meyers (ed.), *Encyclopedia of Analytical Chemistry*, chapter a9070. DOI: 10.1002/9780470027318.a9070 (on line posting date December 15, 2009).

Postma, H. and P. Schillebeeckx 2017. Chapter 12 In: Nikolay Kardjilov and Giulia Festa (eds), *Neutron Methods for Archeology and Cultural Heritage*. Springer International Publishing Switzerland, 235-284. DOI 10.1007/978-3-319-33163-8

Siano, S., L. Bartoli, M. Zoppi, W. Kockelmann, M. Daymond, J.A. Dam, M.G. Garagnani and M. Miccio 2003. Microstructural bronze characterisation by time of flight neutron diffraction. *Proceedings Archaeometallurgy in Europe* 2, 319-329.

Siano, S., L. Bartoli, J.R. Santisteban, W. Kockelmann, M.R. Daymond, M. Miccio and G. De Marinis 2006. Non-destructive investigation of bronze artefacts from the Marches National Museum of Archaeology using neutron diffraction. *Archaeometry* 48, 77.

Schillebeeckx, P., A. Borella, F. Emiliani, G. Gorini, W. Kockelmann, S. Kopecky, C. Lampoudis, M. Moxon, E. Perelli Cippo, H. Postma, N. J. Rhodes, E.M. Schooneveld and C. Van Beveren 2012. Neutron resonance spectroscopy for the characterization of materials and objects. *Journal of Instrumentation* (JINST) 7, 1-18.

Spiridonov, E.M. 2013. *Kostovite Au(Cu, Ag, Au)Te_4 – conditions of formation and replacing minerals in hydrothermal gold deposits*. Bulgarian Geological Society, National Conference with international participation "GEOSCIENCES 2013", 51-52.

Von Quillfeldt, I. 1995. *Die Vollgriffschwerter in Süddeutschland*. Prähistorische Bronzefunde (PBF) IV, 11.

Hans Postma
RD&M
Department of Applied Physics
Delft University of Technology

Mekelweg 15
2629 JB Delft
The Netherlands
postma-bosch@dataweb.nl

Luc Amkreutz
National Museum of Antiquities
PO Box 11114
2301 EC Leiden
The Netherlands
l.amkreutz@rmo.nl

David Fontijn and Hans Kamermans
Faculty of Archaeology
University Leiden
PO Box 9514
2300 RA Leiden
The Netherlands
d.r.fontijn@arch.leidenuniv.nl
h.kamermans@arch.leidenuniv.nl

Winfried A. Kockelmann
ISIS Facility
STFC, Rutherford Appleton Laboratory
Chilton OX11 0QX
UK
winfried.kockelmann@stfc.ac.uk

Peter Schillebeeckx
European Commission, Joint Research Centre
Retieseweg 111
B-2440 Geel
Belgium
peter.schillebeeckx@ec.europa.eu

Dirk Visser
Loughborough University
Department of Physics
Loughborough
UK
d.visser@lboro.ac.uk